Environmental Enrichment Induces Synaptic Structural Modification After Transient Focal Cerebral Ischemia in Rats

XIAOHONG XU,*,†,[1] LINGJING YE,* AND QIN RUAN*,†

*Chemistry and Life Science College, Zhejiang Normal University, Jinhua, Zhejiang 321004, China; and †Ecology Research Institution, Zhejiang Normal University, Jinhua, Zhejiang 321004, China

Environmental enrichment (EE), where animals are exposed to a complex novel environment, has been shown to induce synaptic plasticity in both intact and injured animals. The purpose of this study was to investigate the effects of EE on spatial memory and structural modifications of synaptic junctions in rats following transient focal cerebral ischemia. Adult male Sprague-Dawley rats underwent right middle cerebral artery occlusion (MCAO) for 40 min and reperfusion. On day 3 after MCAO or sham surgery, rats were randomly assigned for 14 days to enriched or standard environmental housing. Spatial memory was then tested by the Morris water maze. Parietal cortex and the CA1 region of hippocampus were processed for electron microscopy and stereological techniques were used to evaluate plasticity of synaptic junctions. EE after MCAO improved spatial memory, with shortened escape length, increased frequency of crossings at the location of the platform, and increased percentage of time spent in the quadrant where the platform was previously located. Synaptic ultrastructural analysis showed that EE after MCAO increased numeric synaptic density in parietal cortex, and induced structural changes in synaptic junctions, with a decreased width of synaptic clefts and increased thickness of postsynaptic densities (PSD) in parietal cortex and hippocampus, accompanying improved performance on the spatial memory task. Using Western blot analysis, we determined the expression of glutamate receptor NMDAR1, and PSD-95, the best characterized protein member of the PSD-95 family, that was abundantly expressed in the PSD of excitatory synapses. The results showed that the content of NMDAR1 was not altered in MCAO rats of EE; however, the phosphorylated NMDAR1 increased significantly when compared with the standard environment housing MCAO rats. In addition, EE inhibited the impaired expression of PSD-95 induced by MCAO in parietal cortex and hippocampus. These data suggest that improved spatial memory of cerebral ischemic rats by EE is associated with structural modifications of synaptic junctions in several brain regions. Exp Biol Med 234:296–305, 2009

Key words: environmental enrichment; cerebral ischemia; synaptic plasticity; NMDA; PSD-95

Introduction

Ischemic brain injury remains one of the most common causes of death and disability throughout the world for which, at present, there is no comprehensive pharmacotherapy (1). In cerebral ischemia, neural plasticity seen in regions that surround the primary injury site includes dendritic restructuring (2–4), reactive synaptogenesis (5), and enhanced neurogenesis (6). Ischemic insult also activates a variety of potential growth-promoting processes including increases in neurotrophic factors (7), and cell adhesion molecules (8). Thus, it is possible that these adaptive changes provide a condition that is highly permissive of behaviorally driven synaptic plasticity. It is well established that environmental enrichment (EE) can induce plastic changes in the brains of intact and post-injury animals. This includes both morphological (e.g., increased number of neurons and synapses), and behavioral changes such as improved learning and memory (9, 10). EE enhances the recovery of both sensorimotor function and memory impairment after stroke in rodents, without decreasing infarct volume (2, 11, 12). This is linked to plastic processes outside the ischemic lesion (9, 13). For rodents, post-ischemic housing in an enriched environment enhances brain-derived neurotrophic factor (BDNF) mRNA and protein expression (14), increases dendrite branching and dendritic spine density (4), enhances synaptogenesis (15), and increases the number of synapses with perforated postsynaptic densities and synaptic terminals that form multiple synapses in the hippocampus or the neocortex (16).

This study was supported by National Science Foundation of China (No. 30771783 and No. 30872087) and Zhejiang Province Natural Science Foundation (M303042).

[1] To whom correspondence should be addressed at Zhejiang Normal University, Chemistry and Life Sciences College, Yinbin Road, Jinhua, Zhejiang 321004, China. E-mail: xuxh63@zjnu.cn

Received April 3, 2008.
Accepted December 23, 2008.

DOI: 10.3181/0804-RM-128
1535-3702/09/2343-0296$15.00

The structural modifications accompanying behavioral training and complex environmental experience reported previously were in the two major categories: changes in pre-existing synapses and changes in the number of synapses (17). The synaptic interface structural modifications in pre-existing synapses have been shown following behavioural trainings and complex environmental experience in the brains of animals (18, 19). Vrensen and Cardozo observed a significant increase in the thickness of the postsynaptic density (PSD) and a decrease in the synaptic cleft in the visual cortex of rabbits after visual training (20). Qiang *et al*. found that the process of learning and memory was not accompanied by alterations in the size of synapses and the number of synaptic vesicles, but significantly induced an increase in the thickness of PSD, and a decrease in the width of the synaptic cleft and the number of local vesicles (19).

PSD is a protein complex that lays postsynaptic membranes at the synaptic contact zone. In addition to postsynaptic receptors, PSD also contains key elements involved in neuronal postsynaptic activity, such as signal- and scaffolding-proteins that organize the functional post-synaptic structure (21). The changes of protein-protein interaction between the receptors and submembranous scaffolding/signaling proteins of the PSD are reflected in the variable postsynaptic activity and plasticity (22–24). These structural modifications are believed to serve as a morphological basis for changes in behavior and cellular activity. PSD-95 (postsynaptic density protein of 95 kDa) is an essential synaptic adaptor protein that is involved in the anchoring of NMDA receptor (NMDAR) subunits. Because the PSD-95 protein plays a central role in the regulation of synaptic function, and is also important in regards to linking of the synapse to downstream signaling pathways (25), the PSD-95 protein could also be involved in the process of hypoxia/ischemia-induced changes that lead to neuronal damage. Thus, we presume that the improvement effects of EE on functional outcome in cerebral ischemic rats may be related to the enhancement in synaptic interface modification in the areas of brain related to behavior. In our previous study, we found that occlusion of the middle cerebral artery (MCAO) for 40 min limited infarcts to the lateral striatum and the lateral cortex (infarct core), and the surrounding cortex (parietal cortex) and hippocampus were moderately hypoperfused (border zone of infarct) (26). In the current study, the changes of synaptic structure and the postsynaptic proteins PSD-95 and NMDA receptor in parietal cortex and hippocampus were investigated to elucidate the mechanism underlying the improvement of EE on functional outcome in cerebral ischemic rats.

Materials and Methods

Preparation of MCAO and Reperfusion Model. All animal handling and surgery were performed in accordance with the Care Standard of the Laboratory Animal (China Ministry of Health publication, 1998). Male Sprague-Dawley rats, weighing 300–350 g, from Zhejiang Academy of Medical Science, were subjected to MCAO as previously described with modification (27). Briefly, the rats were anaesthetized with chloral hydrate (400 mg/kg, ip). The right common carotid artery (CCA), the external carotid artery (ECA) and the internal carotid artery (ICA) were exposed. A nylon monofilament (diameter, 0.234 mm) with a blunted tip was introduced into the ECA lumen, and then gently advanced to the distal ICA until resistance was felt, which ensured the occlusion of the origin of the middle cerebral artery. The distance between the CCA bifurcation and the resistive point was about 19–19.5 mm. During the entire stroke procedure, rectal temperature was controlled at approximately 37.0–37.5°C with a heating pad and light. The filament was withdrawn from the ICA after 40 min to allow MCA reperfusion. Control rats received sham surgery, in which an identical procedure was followed but inserting the filament 5 mm. To monitor occlusion and reperfusion, the local cerebral blood flow (LCBF) was measured using a laser-Doppler blood flowmeter (Periflux 4001, Perimed, Sweden). Two laser-doppler probes were placed on the right side of the dura at 1 mm posterior and 3 mm and 5 mm lateral to the bregma (28). LCBF was calculated as the averaged values during a 1-min period for every 10 min before and during occlusion, and up to 30 min of reperfusion. The right femoral artery was cannulated for monitoring mean arterial blood pressure (MABP) using Blood Pressure Analyzer (Micro-Med, Inc., Louisville, Kentucky).

Neurological Functions. Neurological deficits were evaluated on all sham-operated and MCAO animals at 4 h after reperfusion. Rats were scored on a four-point scale (0–4) described by Zea-Longa *et al*. (0 = no deficit, 1 = failure to extend left forepaw fully, 2 = circling to the left, 3 = falling to the left, 4 = no spontaneous walking with a depressed level of consciousness) (27). The inclusion of an animal in the present study was dependent on neurological score of 2 for MCAO rats (the rate of exclusion is 77.5%, and nine rats were excluded) or 0 for sham-operated rats.

Housing Conditions. On the third day after MCAO, rats were randomly assigned for 14 days to enriched environment housing or standard environment housing. All animals were housed in the same room under a 12 h light/12 h dark cycle and had free access to food and water. Room temperature was maintained at about 22°C and noise level was kept to a minimum. Animals in the enriched environment ($n = 20$ ischemia and $n = 20$ sham) were housed ten per cage (five ischemic and five sham animals) for 14 days. The enriched environment consisted of a cage (2 m × 2 m × 1 m) containing a variety of objects such as toys, wooden blocks, running wheels, Plexiglas tunnels, ladders, plastic castles, swing, etc. In addition, EE rats were placed daily in an open field (diameter 120 cm) where they were allowed to explore a novel arrangement of objects for 10 min during cage changing. Objects in both EE housing and open field were changed daily to maintain novelty. Animals assigned

in the standard environment ($n = 20$ ischemia and $n = 20$ sham) were housed in pairs in standard laboratory cages (29 cm × 21 cm × 34 cm) without any other object than food cages and water bottles. The sham rats housed in standard environment were used as controls.

Morris Water Maze. After EE period, rats were submitted to behavioral testing for the study of spatial memory in the Morris water maze. The maze consisted of a black circular pool with 170 cm in diameter filled with water (temperature 25 ± 1°C) situated in a room with visual cues on the wall. The pool was geographically divided into four equal quadrants, with release points in each quadrant designated as southwest, northwest, northeast, and southeast. A transparent platform (8 cm in diameter) was located 1 cm beneath the water surface. This escape platform location was kept constant in the middle of the southwest quadrant.

In this task the rats ($n = 9$ for each group) were trained to locate a hidden escape platform in the water pool as reported by Wilson *et al*. with modification (29). In brief, rats were placed into the water facing the wall at each of those releasing points in a random order. A video camera mounted above the maze was connected to a computer tracking system (VideoMot2-BWM, TSE Systems GmbH, Germany), and was used to record the swim pattern. The rats were allowed 120 sec to find the submerged platform, and then allowed to stay on the platform for 15 sec. If the rat failed to find the platform in the maximum time (120 sec), the experimenter placed it there for 15 sec. The inter-trail interval was 60 sec. Each rat performed four trials daily for 4 days. During the training trials, path length with which each animal found the platform was measured. On the fifth day, rats were given a 2-min probe trial in which the platform was removed. The start point for the probe trial was randomly selected for each subject. The swimming track of rats was recorded.

Postsynaptic Density (PSD) Preparation. Rats were decapitated after 2 weeks of enriched environment housing or standard environment housing ($n = 5$ for each group); and brains were rapidly removed and placed on an ice-cooled plate for dissection of parietal cortex and hippocampus, and then kept at –80°C until use.

The PSD fraction was prepared as Carlin *et al*. described (30) with some modifications. Parietal cortex and hippocampus were homogenized in 4 volumes of ice-cold buffer containing 0.32 M sucrose, 1 mM $MgCl_2$ and 1 μg/ml leupeptin in 1 mM of HEPES (pH 7.4) using a Potter-Elvehjem tissue grinder with Teflon pestle, and synaptosomes were obtained by differential and density gradient centrifugations as follows: sucrose gradients containing 8 ml of the resuspended brain preparation and gradients containing 10 ml each of 1.25 M, 1.0 M and 0.85 M sucrose solutions were centrifuged for 2 h at 80,000 × *g* (Beckman Instruments). The synaptosomal fraction was collected from the interface of 1.25 M and 1.0 M sucrose and diluted with 1 mM of HEPES, pH 7.4, to 11 ml/g of original tissue. An equal volume of 1% Triton X-100 in 0.32 M sucrose was added and stirred at 4°C for 15 min. This suspension was centrifuged at 36,000 × *g* for 30 min and the pellets were resuspended into 0.32 M sucrose (0.4 ml/g of original tissue). Two milliliters of this material layered onto gradients in polyallomer tubes containing 4 ml of 2.1 M sucrose and 3 ml each of 1.5 M and 1.0 M sucrose. The gradients were centrifuged for 2 h at 200,000 × *g* (Beckman Instruments). The postsynaptic fraction was collected from the 2.1–1.5 M interface with a siliconized plastic pipette and diluted with 20 mM of HEPES and an equal volume of 1% Triton X-100 in 150 mM KCl to obtain 0.5 ml/g of original tissue. The PSD fraction was collected on the 2.1 M sucrose cushion by centrifugation at 200,000 × *g* for 40 min. This interface was then resuspended in 20 mM HEPES, pH 7.4, and again collected on the 2.1 M sucrose by centrifugation at 200,000 × *g* for 30 min. The PSD fraction from the interface was resuspended by stirring in 40% glycerol. The protein content of PSD fraction was estimated by a BCA assay (Pierce, Rockford, IL).

Western Blotting. For Western blots, proteins were separated by 7.5% SDS-PAGE mini-gels after heating samples at 90–100°C for 5 min, and transferred to nitrocellulose membrane using a Trans-Blot system (Bio-Rad, Hercules, CA). Anti-NMDAR1 (NMDA receptor subunits type 1; 1:300) and anti-phospho-NMDAR1 ser^{896} (phosphorylated subunits of NMDA receptor type 1; 1:1000) antibodies were obtained from Chemicon (Temecula, CA, USA) and Upstate Biotechnology (Lake Placid, NY, USA), respectively. Antibody against PSD-95 (1:5000) was obtained from ABR (Golden, CO, USA). Immunoblots were scanned, and the digitized images were analyzed quantitatively by densitometry with a computer image analysis system (Quantity One, Bio-Rad Laboratories).

Electron Microscopic Preparations and Morphometric Measurement. After 2 weeks of enriched environment housing or standard environment housing, rats were anesthetized with an overdose of chloral hydrate and intercardially perfused with 0.9% saline followed by 0.1 M phosphate buffer containing 4% paraformaldehyde and 1.5% glutaraldehyde. The brains were exposed and the samples were taken from both sides of parietal cortex (B: 0.6 to –0.4 mm) and hippocampal CA1 (B: –3.0 to –4.0 mm), according to the atlas of Paxinos and Watson (28) (Fig. 1). Tissues were processed for transmission electron microscopy routinely (19). To ensure consistency between groups in procedures that may affect tissue shrinkage and section thickness, tissue from all groups was processed together for each step of histological processing. The ultrathin sections (approx. 65 nm thick) were initially examined at ×3000 in a H-600 TEM (Hitachi, Japan) electron microscope in order to locate the areas for investigation: the external pyramidal cell layer of parietal cortex and the stratum radiatum of CA1 (~75–100 μm away from the stratum pyramidale) that receives Schaffer collateral input.

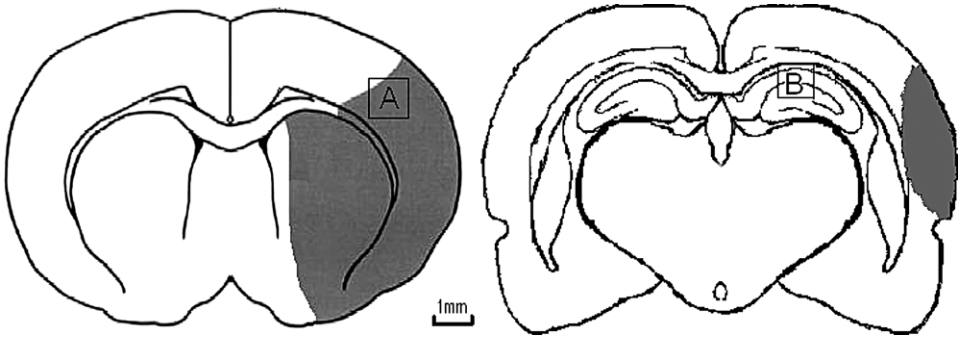

Figure 1. Location of cerebral ischemia (infarcted tissue is shown in gray) and regions sampled for electromicrographs: parietal cortex (A) and hippocampus (B).

Synapses are classified asymmetric and symmetric synapses, or Gray I type and Gray II type synapses, which are considered to mediate excitatory and inhibitory transmission respectively (31). Asymmetric synapses (Gray I type) with prominent post-synaptic densities and relatively wide synaptic clefts (approx. 20 nm), while symmetric synapses (Gray II type) with pre- and post-synaptic densities of equal thickness and narrower synaptic clefts (approx. 12 nm). In the present study, Type I synapses of Gray were examined for synaptic measurement. Type I synapses of Gray were identified by the presence of presynaptic and postsynaptic membrane apposition, synaptic cleft, PSD, and at least three vesicles in the presynaptic bouton (16) (Fig. 2).

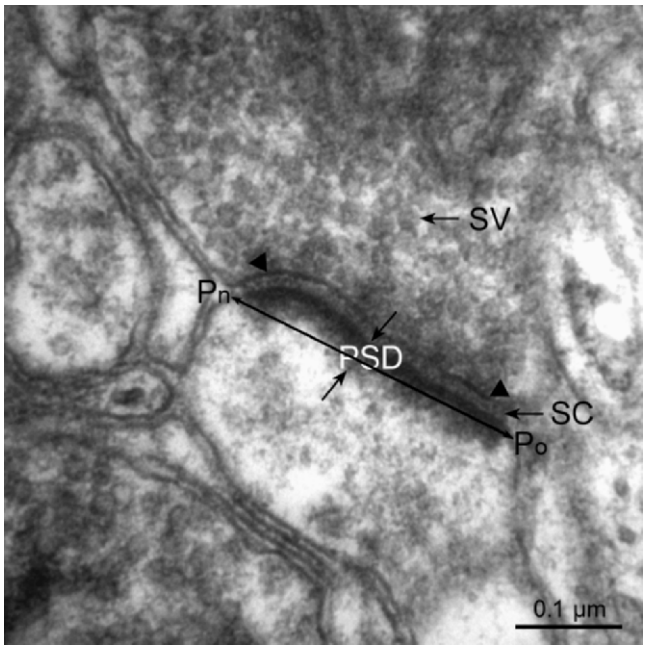

Figure 2. Electromicrographs showing the ultrastructural features of synapses in hippocampus CA1 area. The limits of the length of synaptic active zone were indicated by two arrowheads. The thickness of postsynaptic density (PSD) was at the thickest part of PSD and limited by two long arrowheads; Po and Pn showed the synaptic curvature measurement points; SC represents the synaptic cleft (the mean of three values including the largest, middle, and smallest); SV represents synaptic vesicles.

The width of synaptic cleft (the mean of three values including the largest, middle, and smallest), the thickness of PSD at the thickest part, the length of the active zones (Fig. 2), and the curvature (Fig. 3) of the synaptic interface (19) were examined using a graph analyzer (Chendu, China). Electronmicrographs of synapses were taken at magnification of 25,000. Approximately 60 micrographs of each group were examined, and six animals were included in each group. The rats used for the anatomical/immunocytochemical parts of the study were not used in the water maze test.

The dissector technique proposed by Gundersen (32) was adopted in the present study for estimation of numeric

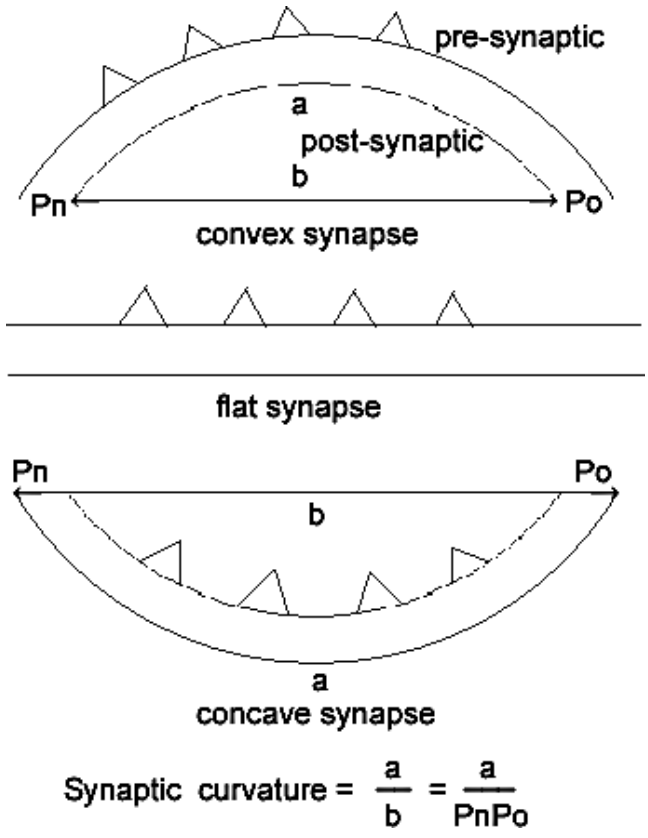

Figure 3. Three types of the synaptic interface and the synaptic curvature measurement.

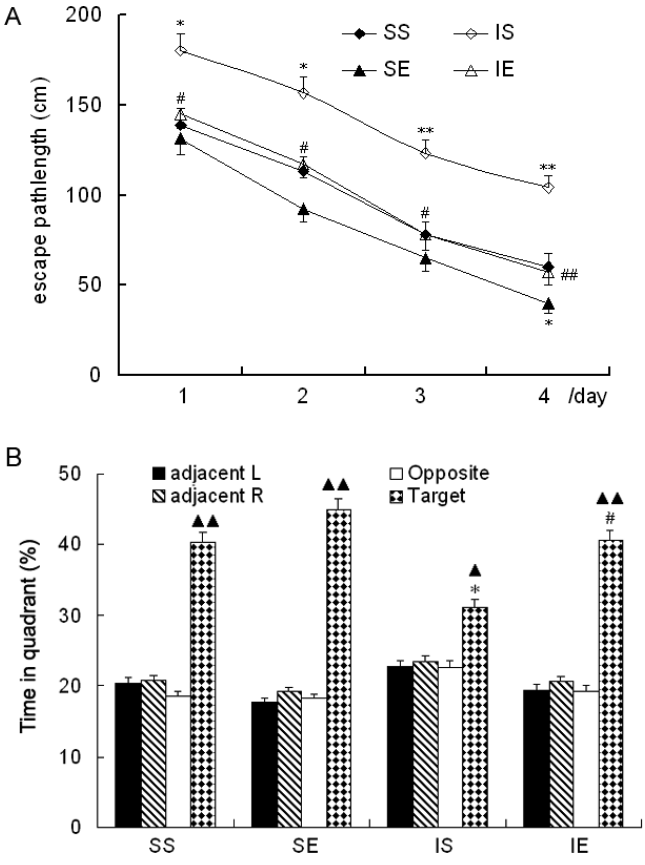

Figure 4. Environmental enrichment significantly improved acquisition of the spatial task. Swim distance (A) was recorded during the platform trials of the spatial water maze task (trials 1–4 of each session). Each point represents the mean ± SEM of each group for trials 1–4. (B) Percentages of time spent in the pool quadrants were recorded and calculated. All groups showed an increased preference (▲ $P < 0.05$ or ▲▲ $P < 0.01$, compared with any of the other quadrants) to search the target quadrant where the platform used to be. SS, sham rats of standard environment housing; SE, sham rats of enriched environment housing; IS, ischemic rats of standard environment housing; IE, ischemic rats of enriched environment housing. $n = 9$ for animals. * $P < 0.05$, compared with SS; # $P < 0.05$, compared with IS.

synaptic densities. Briefly, 15–25 pairs of adjacent ultrathin sections were analyzed from parietal cortex and hippocampal CA1 of each animal. In each pair of sections, two unbiased disector frames (6–5 μm) were arranged in a pseudo-random fashion. The first section was considered the 'reference' and the second, the 'look-up' section. Within the frame, the number of synapses that were present in the 'reference' section and absent in the 'look-up' section (Q^-) was counted. Each section was used as both 'reference' and 'look-up' sections in a way that synapses were counted as they disappear while moving in both directions through the series of sections. The dissector volume of tissue within which the synapses were counted (V_{dis}) was estimated as $V_{dis} = A_{frame}tn$, where A_{frame} is the unbiased counting frame, t is section thickness (65 nm, based on microtome settings), and n is the number of sections through which the counting was done. Synaptic density was then calculated as: $Nv = Q^-/V_{dis}$. The number of animals was six in each group.

Statistical Analysis. The data were expressed as mean ± SEM. The effects of housing conditions and training upon water maze performance were evaluated by two-way repeated measure ANOVA. Difference between groups was then tested using the Tukey's test. Statistical analysis of the optical densities (OD) and morphometric measurement was performed by Tukey's test following one-way ANOVA. The statistical significance was accepted at $P < 0.05$.

Results

In the experiment, 40 min MCAO induced an immediate reduction of LCBF in the border and core of infarction. The mean LCBF were 26.3 ± 3.4% and 42.1 ± 4.5% of baseline ($P < 0.01$) in the core and the border, respectively, during the ischemic period. Following withdrawal of the intra-luminal suture, LCBF recovered to 70–85% of baseline and gradually returned to baseline level 30 min after reperfusion. Though MABP slightly rose during ischemia, it was not statistically different from that before MCAO.

Morris Water Maze. MCAO did not impair the velocity in the Morris water maze, but severely impaired spatial memory in rats. The average distance to reach the platform (escape length) was significantly increased in the MCAO rats during the training period of 4 consecutive days when compared to sham rats ($P < 0.01$). However, housing in the enriched environment shortened the escape length not only in MCAO rats but also in sham rats. On test day 4, the escape length in MCAO rats of enriched environment (IE) housing was significantly shortened by 45.3% when compared with those of standard environment (IS) housing ($P < 0.01$), and shortened by 34.1% in sham rats of enriched environment (SE) housing when compared with those of standard environment (SS) housing ($P < 0.05$). Moreover, the SE has a shorter escape length when compared to IE (Fig. 4A).

The results of the probe trials showed that all rats demonstrated normal memory retention during the probe trial (with hidden platform removed) of the water maze training, because all groups showed an increased preference to search for the target quadrant where the platform was previously located when compared with any of the other quadrants (Fig. 4B). However, the frequency of crossings where the platform had been and the percentage of time spent in the quadrant where the platform had been during training, were obviously decreased in MCAO rats when compared to sham rats ($P < 0.05$) (Fig. 4B). After enriched environment housing for 14 days, the frequency of crossings in the quadrant where the platform was previously located and the percentage of time spent in the quadrant where the platform was previously located, were increased in MCAO rats ($P < 0.05$) (Fig. 4B).

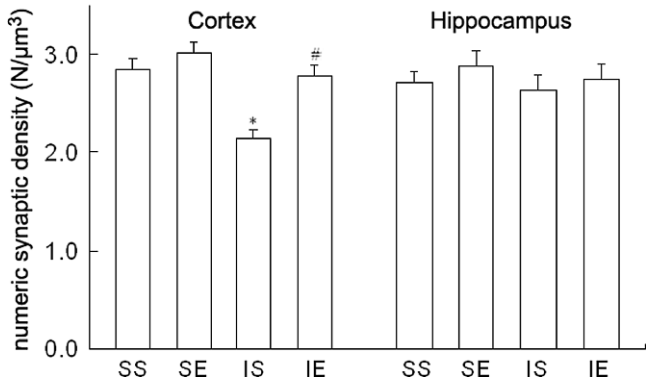

Figure 5. Effects of environmental enrichment on numeric synaptic density ($N/\mu m^3$) in dorsolateral cortex and hippocampus CA1 areas of MCAO and sham rats. The results are expressed as mean ± SEM, $n = 6$ for animals. SS, sham rats of standard environment housing; SE, sham rats of enriched environment housing; IS, ischemic rats of standard environment housing; IE, ischemic rats of enriched environment housing. * $P < 0.05$, compared with SS; # $P < 0.05$, compared with IS.

Synaptic Ultrastructural Measurement and Analysis. The synaptic numeric density (N_V) was not affected in the hippocampus, but significantly decreased in parietal cortex ($P < 0.05$) after MCAO (Fig. 5). In addition, some of the structural parameters of the synaptic junction were altered by MCAO (Fig. 6), with a widened synaptic cleft, a thinned PSD, and a shortened synaptic active zone in both parietal cortex and hippocampus. EE inhibited the structural alterations induced by MCAO. Compared with IS, EE attenuated MCAO-induced decrease in the synaptic numeric density by 26.8% ($P < 0.05$) (Fig. 5) in parietal cortex, declined the width of synaptic cleft by 16.4% ($P < 0.05$) in parietal cortex and by 15.2% ($P < 0.05$) in hippocampus, increased the thickness of PSD by 22.9% ($P < 0.05$) in parietal cortex and by 24.1% in hippocampus ($P < 0.01$) (Fig. 6). The enhanced effects of EE on synaptic junction structure were also observed in sham rats, with a decreased synaptic cleft width and increased thickness of the PSD in parietal cortex ($P < 0.05$ and $P < 0.05$) and in hippocampus ($P < 0.05$ and $P < 0.01$); the SE had the thinnest synaptic cleft and the thickest PSD among the groups (Fig. 6). The

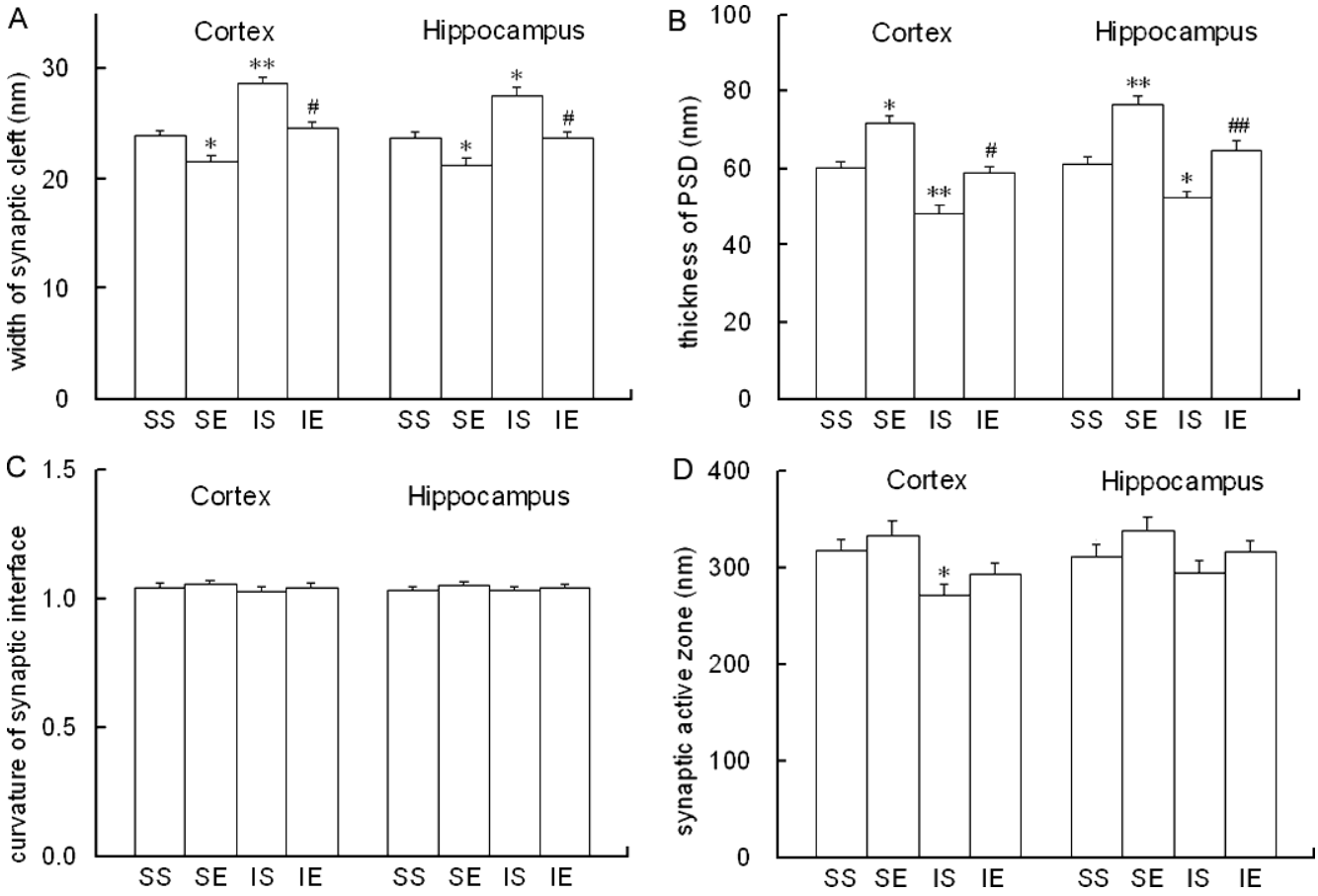

Figure 6. Effects of environmental enrichment on the structural modification of synaptic interface in dorsolateral cortex and hippocampus CA1 areas of MCAO and sham rats. (A) The width of synaptic cleft; (B) the thickness of PSD; (C) the curvature of synaptic interface; (D) the length of synaptic active zone. The results are expressed as mean ± SEM, $n = 60$ for synapses. The number of animals was 6 in each group. SS, sham rats of standard environment housing; SE, sham rats of enriched environment housing; IS, ischemic rats of standard environment housing; IE, ischemic rats of enriched environment housing. * indicates that the value differs from SS at $P < 0.05$ and ** indicates $P < 0.01$; # indicates that the value differs from IS at $P < 0.05$ and ## indicates $P < 0.01$.

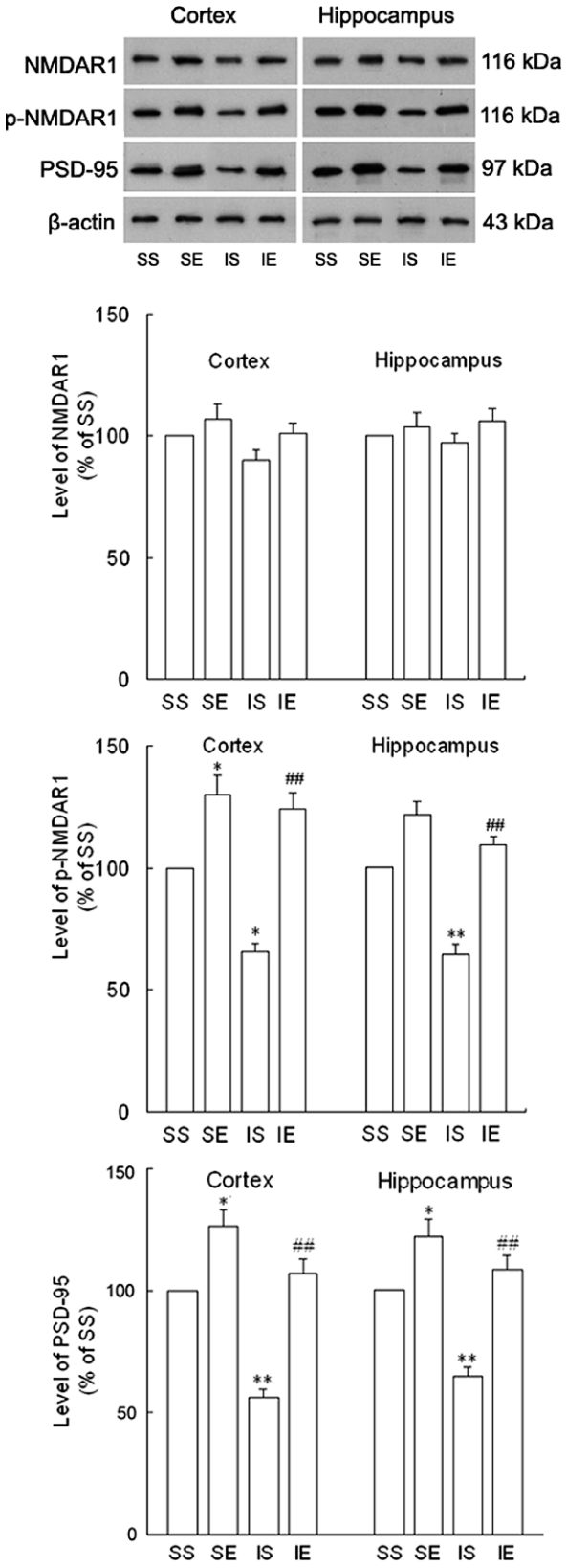

Figure 7. Effects of environmental enrichment on the immunocontent of PSD proteins in dorsolateral cortex and hippocampus of MCAO and sham rats. Western blot and quantification of band intensity are shown. Results are mean ± SEM, $n = 5$ tissue preparations for all experiments. SS, sham rats of standard environment housing; SE, sham rats of enriched environment housing; IS, ischemic rats of standard environment housing; IE, ischemic rats of enriched environment housing. * indicates that the value differs from SS at $P < 0.05$ and ** indicates $P < 0.01$; ## indicates that the value differs from IS at $P < 0.01$.

other synaptic junction structural parameters, such as the curvature of synaptic interface and the synaptic active zone, were not significantly different between the EE housing and standard environment housing groups ($P > 0.05$).

The Immunocontent of Postsynaptic Proteins. Since the number and the activity of NMDA receptor are associated with glutamatergic synaptic strength, and the phosphorylation of NMDA receptor subunits affects the receptor's activity, the immunocontent of NMDAR1 and phosphorylated NMDAR1 in parietal cortex and hippocampus were assessed, aiming to better characterize the effects of EE on synaptic modification in MCAO rats. There were no statistically significant differences in the immunocontent of NMDA1 between sham and MCAO rats; however, phosphorylated NMDA receptor subunit, phospho-Ser^{896}-NMDAR1 was reduced by MCAO in both parietal cortex ($P < 0.05$) and hippocampus ($P < 0.01$) (Fig. 7). EE did not affect the immunocontent of NMDAR1, but increased the phosphorylation of NMDAR1 of these brain regions, especially in MCAO rats (Fig. 7). In addition to postsynaptic receptors, PSD also contains signaling- and scaffolding-proteins that organize the functional postsynaptic structure (33). Thus, we also quantified PSD protein PSD-95, which anchor glutamate receptors. The results showed that MCAO markedly decreased immunocontent of PSD-95 in parietal cortex and hippocampus ($P < 0.05$) when compared to the sham rats (Fig. 7). EE inhibited the down-regulation of PSD-95 in protein level induced by MCAO, with a promoted immunocontent by 88% ($P < 0.01$) in parietal cortex and by 75% ($P < 0.01$) in hippocampus when compared to MCAO rats housing in standard environment. In addition, EE increased immunocontent of PSD-95 protein ($P < 0.05$) of both brain regions in sham rats.

Discussion

The main findings of the present study are that: (i) along with enhanced functional recovery, surviving neurons in parietal cortex and hippocampal regions of the adult rat continue to exhibit synaptic plasticity after transient focal cerebral ischemia, evidenced by significant structural modifications in the synaptic junctions after behavioral experience in the enriched environment; and (ii) EE increased expressions of phosphorylated NMDAR1 and PSD-95 in parietal cortex and hippocampal regions surrounding the primary site of injury resulted from transient focal cerebral ischemia. Improved spatial learning, increased structural synaptic plasticity and expression of postsynaptic proteins seen in the sham rats from the

enriched environment in the present study are an expected finding given previous reports that behavioral experience in a complex environment appears to benefit cortical plasticity and learning abilities at any point in the lifespan (9, 34).

Environmental enrichment (EE), as a stimulation paradigm, involves a combination of increased social interaction, physical exercise and continuous exposure to learning tasks and produces interesting effects (35). It has been reported that experience in the complex environment following ischemic injuries enhanced neural plasticity, including enhanced neurogenesis, dendritic restructuring and reactive synaptogenesis (36). Ultrastructural changes, such as increased synapses with multiple synaptic boutons and dendritic spine density, were also found in cerebral ischemic rats after experience in the complex environment (15). In the present study, we also found an increased synaptic numeric density in parietal cortex of MCAO rats after EE housing. However, it remains unclear so far whether the structure of synaptic interface altered following EE in MCAO rats. Thus, in this study, we examined the effects of enriched environment exposure after transient focal cerebral ischemia on structural modification in synaptic junctions. The results of the present study showed that the structural alterations of synaptic interface, including a widened synaptic cleft and a thinned PSD induced by MCAO, were attenuated following post-ischemic housing in enriched environment. The structural modifications of synaptic junctions in pre-existing synapses are important for synaptic transmissive efficiency alteration. Previous studies found that learning and memory impairments were accompanied by a decreased thickness of the PSDs and increased synaptic cleft width (37). Long-lasting LTP induced increases in synaptic junctions curvature and PSD thickness, as well as decrease in the cleft width (18). EE housing increased PSD length in the visual cortex (7). Our results suggest that EE not only increases the synaptic numeric density but also modulates structural modifications of synaptic junctions outside the ischemic lesion in cerebral ischemic rats, and the improved spatial memory of MCAO may be associated with the enhanced synaptic structural plasticity in areas adjacent to the injury site after EE.

The PSD has long been considered to be made up of a mixture of proteins, such as cytoskeletal and scaffold proteins, glutamate receptors, calmodulin binding protein, ion channels, and signaling molecules (38). It is becoming increasingly clear that the PSD is a dynamic structure whose morphology and composition change with activity, reflecting trafficking and reorganization of its components (39). The interactions of post-synaptic proteins are involved in neuronal differentiation, synaptogenesis, synaptic plasticity and the processes of learning and memory (40–42). Changes in the abundance and organization of PSD components as well as their functional modification are likely to be mediated, at least in part, through changes in the phosphorylation states of proteins. NMDA receptors exert a key role in neuronal excitability and synaptic signaling through a fine control of its channel activity. Accordingly, phosphorylation of NMDA receptors increases the ion current through the receptor, whereas their activity decreases by action of protein phosphatases (21). It has been suggested that NMDA receptors activity is an essential step to experience-induced synaptic plasticity in hippocampus (43). Therefore, the increased phosphorylation of NMDAR1 and unchanged immunocontent of NMDAR1 in parietal cortex and hippocampus of MCAO rats following EE in the present study, suggest increased NMDA receptor activity by EE.

PSD-95 is the best characterized protein member of PSD-95 family, which anchors receptors, maintaining the architecture and functionality of the PSD (44). Our present results showed that the immunocontent of PSD-95 accompanied the increase in phosphorylation of NMDAR1 following EE in both sham and MCAO rats. Previous studies support the importance of PSD-95 proteins in synaptic plasticity and in the control of synaptic strength. In rodent hippocampal neurons where PSD-95 was overexpressed, both the density of dendritic spines and the amplitude of miniature excitatory postsynaptic currents were increased (45). The phenotype of PSD-95 mutant mice presented with impaired spatial learning abilities and altered LTP (39). Behavioral training increased the immunocontent of PSD-95 protein (43, 46). Increases in PSD-95 gene expression or protein levels have also been detected in cortex and hippocampus following EE and other experimental manipulations, which induce synaptic plasticity (33). In addition, it was found that perinatal hypoxia resulted in the impaired expression of the PSD-95 protein in the hippocampal CA1 region of rats (25). Altered PSD-95 expression was also involved in hypoxia-induced changes leading to neuronal injury for the adult brain (23, 47). In the present study, we found that the thickness of PSD and immunocontent of PSD-95 in both parietal cortex and hippocampus of MCAO rats were markedly decreased, while the synaptic numeric density did not change in the hippocampus. This suggests that the decreased expression of PSD-95 is associated with the thinned PSD but not lost synapses in the MCAO rats. EE increased the thickness of the PSDs as well as increased the expression of PSD-95 in the MCAO rats.

It has been suggested that PSD-95 through its multiple protein interaction domains can mediate the association of NMDAR with different downstream signaling elements, thereby regulating bi-directional synaptic plasticity (21). Moreover, it has been shown that activity-dependent synaptic plasticity can modulate PSD-95 association with NMDAR thus affecting the dynamic interactions between CaMKII, PSD-95 and NMDAR (48). Chen *et al*. found that perinatal hypoxia resulted in a decreased protein expression for the PSD-95 and total NMDAR level, as well as a reduced interaction between PSD-95 and NMDAR subunits (25). Hypoxia-ischemia activated calpain, a calcium-dependent protease, truncating the C-terminal domain of

NMDAR subunits, thereby resulting in the loss of the ability of the subunits to bind to PSD-95 for adult animals (22). These findings together with the present results raise the possibility that EE enhances protein-protein interactions between PSD-95 and postsynaptic proteins, such as NMDA receptors, thereby contributing to structural modification of synaptic interface and improved learning and memory of cerebral ischemic rats. The answers provided by this research in rodents will be hopeful for further studies on the neurobiological mechanisms of recovery of cognitive functions after ischemic stroke.

1. Kidwell CS, Liebeskind DS, Starkman S, Saver JL. Trends in acute ischemic stroke trials through the 20th century. Stroke 32:1349–1359, 2001.
2. Biernaskie J, Corbett D. Enriched rehabilitative training promotes improved forelimb motor function and enhanced dendritic growth after focal ischemic injury. J Neurosci 21:5272–5280, 2001.
3. Carmichael S. Plasticity of cortical projections after stroke. Neuroscientist 9:64–75, 2003.
4. Johansson BB, Belichenko PV. Neuronal plasticity and dendritic spines: effect of environmental enrichment on intact and postischemic rat brain. J Cereb Blood Flow Metab 22:89–96, 2002.
5. Horner CH, Davies HA, Brown J, Stewart MG. Reduction in numerical synapse density in chick (Gallus domesticus) dorsal hippocampus following transient cerebral ischemia. Brain Res 735:354–359, 1996.
6. Kee NJ, Preston E, Wojtowicz JM. Enhanced neurogenesis after transient global ischemia in the dentate gyrus of the rat. Exp Brain Res 136:313–320, 2001.
7. Klintsova AY, Greenough WT. Synaptic plasticity in cortical synapses. Curr Opin Neurobiol 9(2):203–208, 1999.
8. Cotman CW, Hailer NP, Pfister KK, Soltesz I, Schachmer M. Cell adhesion molecules in neural plasticity and pathology: similar mechanisms, distinct organizations? Prog Neurobiol 55:559–569, 1998.
9. Johansson BB. Brain plasticity in health and disease. Keio J Med 53: 231–246, 2004.
10. Briones TL, Klintsova AY, Greenough WT. Stability of synaptic plasticity in the adult rat visual cortex induced by complex environment exposure. Brain Res 1018:130–135, 2004.
11. Dahlqvist P, Rönnbäck A, Bergström SA, Söderström I, Olsson T. Environmental enrichment reverses learning impairment in the Morris water maze after focal cerebral ischemia in rats. Eur J Neurosci 19(8): 2288–2298, 2004.
12. Belayev A, Saul I, Liu Y, Zhao W, Ginsberg MD, Valdes MA, Busto R, Belayev L. Enriched environment delays the onset of hippocampal damage after global cerebral ischemia in rats. Brain Res 964:121–127, 2003.
13. Calabresi P, Centonze D, Pisani A, Cupini LM, Bernardi G. Synaptic plasticity in the ischaemic brain. Neurol 2:622–629, 2003.
14. Gobbo OL, O'Mara SM. Impact of enriched-environment housing on brain-derived neurotrophic factor and on cognitive performance after a transient global ischemia. Behav Brain Res 152:231–241, 2004.
15. Briones TL, Suh E, Jozsa L, Woods J. Behaviorally induced synaptogenesis and dendritic growth in the hippocampal region following transient global cerebral ischemia are accompanied by improvement in spatial learning. Exp Neurol 198:530–538, 2006.
16. Briones TL, Suh E, Jozsa L, Hattar H, Chai J, Wadowska M. Behaviorally-induced ultrastructural plasticity in the hippocampal region after cerebral ischemia. Brain Res 997:137–146, 2004.
17. Briones TL, Suh E, Jozsa L, Rogozinska M, Woods J, Wadowska M. Changes in number of synapses and mitochondria in presynaptic terminals in the dentate gyrus following cerebral ischemia and rehabilitation training. Brain Res 1033:51–57, 2005.
18. Pan B, Yang DW, Han TZ. Changes of synaptic structure after long-lasting LTP induced by high and low frequency tetanus in slices of the rat visual cortex. Acta Physiologica Sinica 57:77–82, 2005.
19. Qiang M, Wang SD, Wu FM, Xie JP, Qiao JT. Involvement of NMDA in synaptic plasticity following behavioral trainings in rats: an ultrastructural study. Chin J Neurosci 16:185–191, 2000.
20. Vrensen G, Cardozo NJ. Changes in size and shape of synaptic connections after visual training: an ultrastructural approach of synaptic plasticity. Brain Res 218:79–97, 1981.
21. Sheng M, Pak DT. Glutamate receptor anchoring proteins and the molecular organization of excitatory synapses. Ann N Y Acad Sci 868: 483–493, 1999.
22. Ostwald K, Hagberg H, Andine P, Karlsson JO. Upregulation of calpain activity in neonatal rat brain after hypoxic-ischemia. Brain Res 630:289–294, 1993.
23. Hu BR, Park M, Martone ME, Fischer WH, Ellisman MH, Zivin JA. Assembly of proteins to postsynaptic densities after transient cerebral ischemia. J Neurosci 18(2):625–633, 1998.
24. Wyneken U, Marengo JJ, Villanueva S, Soto D, Sandoval R, Gundelfinger ED, Orrego F. Epilepsy-induced changes in signaling systems of human and rat postsynaptic densities. Epilepsia 44:243–246, 2003.
25. Chen WF, Chang H, Wong CS, Huang LT, Yang CH, Yang SN. Impaired expression of postsynaptic density proteins in the hippocampal CA1 region of rats following perinatal hypoxia. Exp Neurol 204:400–410, 2007.
26. Xu XH, Zhang SM, Yan WM, Li XR, Zhang HY, Zheng XX. Development of cerebral infarction, apoptotic cell death and expression of X-chromosome-linked inhibitor of apoptosis protein following focal cerebral ischemia in rats. Life Sci 78:704–712, 2006.
27. Zea-Longa E, Weinstein PR, Carlson S, Cummins R. Reversible middle cerebral artery occlusion without craniectomy in rats. Stroke 20(1):84–91, 1989.
28. Paxinos G, Watson C. The Rat Brain in Stereotaxic Coordinates (4th ed.). San Diego: Academic Press, 1998.
29. Wilson IA, Puolivali J, Heikkinen T, Riekkinen PJ. Estrogen and NMDA receptor antagonism: effects upon reference and working memory. Eur J Pharmacol 381:93–99, 1999.
30. Carlin RK, Grab DJ, Cohen RS, Siekevitz P, Isolation and characterization of postsynaptic densities from various brain regions—enrichment of different types of postsynaptic densities. J Cell Biol 86:831–843, 1980.
31. Cuillery RW. Early electron microscopic observations of synaptic structures in the cerebral cortex: a view of the contributions made by George Gray (1924–1999). Trends Neurosci 23(12):594–598, 2000.
32. Gundersen HJ, Bagger P, Bendtsen TF, Evans SM, Korbo L, Marcussen N. The new stereological tools: disector, fractionator, nucleator and point sampled intercepts and their use in pathological research and diagnosis. APMIS 96:857–881, 1988.
33. Nithianantharajah J, Levis H, Murphy M. Environmental enrichment results in cortical and subcortical changes in levels of synaptophysin and PSD-95 proteins. Neurobiol Learn Mem 81:200–210, 2004.
34. Will B, Galani R, Kelche C, Rosenzweig MR. Recovery from brain injury in animals: relative efficacy of environmental enrichment, physical exercise or formal training. Prog Neurobiol 72(3):167–182, 2004.
35. Pereira LO, Arteni NS, Petersen RC, Rocha AP, Achaval M, Netto CA. Effects of daily environmental enrichment on memory deficits and brain injury following neonatal hypoxia-ischemia in the rat. Neurobiol Learn Mem 87:101–108, 2007.
36. Matsumori Y, Hong SM, Fan Y, Kayama T, Hsu CY, Weinstein PR, Liu J. Enriched environment and spatial learning enhance hippocampal

neurogenesis and salvages ischemic penumbra after focal cerebral ischemia. Neurobiol Dis 22:187–198, 2006.

37. Zhang Z, Shen X, Xu X, Wu F. Significance of PSD to memory recession of agedness. Chin J Gerontol 24:332–333, 2003.
38. Kornau HC, Schenker LT, Kennedy MB, Seeburg PH. Domain interaction between NMDA receptor subunits and the postsynaptic density protein PSD-95. Science 269:1737–1740, 1995.
39. Jaffe H, Vinade L, Dosemeci A. Identification of novel phosphorylation sites on postsynaptic density proteins. Biochem Biophys Res Commun 321:210–218, 2004.
40. Migaud M, Charlesworth P, Dempster M, Webster LC, Watabe AM, Makhinson M, He Y, Ramsav MF, Morris RG, Morrison JH, O'Dell TJ, Grant SG. Enhanced long-term potentiation and impaired learning in mice with mutant postsynaptic density-95 protein. Nature 396:433–439, 1998.
41. Yamada Y, Chochi Y, Takamiya K, Sobue K, Inui M. Modulaton of the channel activity of the ε2/ζ1-subtype N-methyl-D-asparate receptor by PSD-95. J Biol Chem 274:6647–6652, 1999.
42. Yao WD, Gainetdinov RR, Arbuckle MI, Sotnikova TD, Cyr M, Beaulieu JM, Torres GE, Grant SG, Cardn MG. Identification of PSD-95 as regulator of dopamine-mediated synaptic and behavioral plasticity. Neuron 41:625–638, 2004.
43. Dietrich MO, Mantese CE, Porciuncula LO, Ghisleni G, Vinade L, Souza DO, Portela LV. Exercise affects glutamate receptors in postsynaptic densities from cortical mice brain. Brain Res 1065:20–25, 2005.
44. Niethammer M, Kim E, Sheng M. Interaction between the C terminus of NMDA receptor subunits and multiple members of the PSD-95 family of membrane-associated guanylate kinases. J Neurosci 16:2157–2163, 1996.
45. Abe K, Chisaka O, Van Roy F, Takeichi M. Stability of dendritic spines and synaptic contacts is controlled by alpha N-catenin. Nat Neurosci 7(4):357–363, 2004.
46. Pollak DD, Herkner K, Hoeger H, Lubec G. Behavioral testing upregulates pCaMKII, BDNF, PSD-95 and egr-1 in hippocampus of FVB/N mice. Behav Brain Res 163:128–135, 2005.
47. Takagi N, Logan R, Teves L, Wallace MC, Gurd JW. Altered interaction between PSD-95 and NMDA receptor following transient global ischemia. J Neurosci 74:169–178, 2000.
48. Gardoni F, Schrama LH, Kamal A, Gispen WH, Cattabeni F, Di Luca M. Hippocampal synaptic plasticity involves competition between Ca^{2+}/calmodulin-dependent protein kinase II and postsynaptic density 95 for binding to the NR2A subunit of the NMDA receptor. J Neurosci 21:1501–1509, 2001.